water

MDPI

Article

Comparison of Saturated Hydraulic Conductivity Estimated by Three Different Methods

Hyoun-Tae Hwang [1,2], Sung-Wook Jeen [3], Ayman A. Suleiman [4] and Kang-Kun Lee [5,*]

1 Aquanty, Inc., 564 Weber Street North, Unit 2, Waterloo, ON N2L 5C6A, Canada; hthwang@aquanty.com
2 Department of Earth and Environmental Sciences, University of Waterloo, Waterloo, ON N2L 3G1, Canada
3 Department of Earth and Environmental Sciences & The Earth and Environmental Science System Research Center, Chonbuk National University, Jeonju-si 54896, Korea; sjeen@jbnu.ac.kr
4 Land, Water and Environment Department, Faculty of Agriculture, The University of Jordan, Amman 11942, Jordan; ayman.suleiman@ju.edu.jo
5 School of Earth and Environmental Sciences, Seoul National University, 1 Gwanak-ro, Gwanak-gu, Seoul 08826, Korea
* Correspondence: kklee@snu.ac.kr; Tel.: +82-2-873-3647

Received: 7 November 2017; Accepted: 1 December 2017; Published: 4 December 2017

Abstract: This study compares saturated hydraulic conductivities (K_s) of three sandy soils such as coarse, medium and fine sand. The K_s was obtained using three different methods: empirical methods based on the grain size analysis, the relative effective porosity model (REPM), and breakthrough curve analyses based on tracer tests. Column drainage tests were performed to characterize the water retention properties of the samples, which are required in the REPM. Bench scale tracer tests with various conditions were conducted to obtain reasonable linear velocities of the samples using breakthrough curve analyses and then K_s was estimated using Darcy's law. For the REPM, the differences of K_s for the coarse and fine sand soils were less than one order of magnitude; however, the difference of K_s values between the empirical methods and the breakthrough curve analyses was larger than one order of magnitude. The comparison results suggest that the REPM can be a reliable method for estimating K_s for soil grains, and is cost effective due to its experimental simplicity.

Keywords: hydraulic conductivity; relative effective porosity model; breakthrough curve analysis; grain size analysis

1. Introduction

It is necessary to obtain appropriate hydraulic parameters such as saturated hydraulic conductivity (K_s) to simulate groundwater flow and solute transport in both saturated and unsaturated conditions, as well as to analyze the soil water dynamics of vertical and lateral drainage flow [1–11]. The soil K_s can generally be measured through field and laboratory experiments (e.g., pumping and permeameter tests) [12]. Neural network analyses combined with stochastic methods have been applied for predicting saturated and unsaturated hydraulic parameters [10,13–17]. According to Bagarello et al. [18], the pressure and the tension infiltrometer methods are widely used as field measurements, and the constant heads and falling heads permeameters and the grain size analysis are generally used as laboratory methods for estimating soil properties including K_s. However, such field and laboratory methods are relatively expensive in terms of duration and cost (e.g., [19,20]).

Alternatively, several methods have been developed to estimate K_s from other physical properties (e.g., [19,21,22]). For example, in 2001 Suleiman and Ritchie [20] proposed a simple model called the relative effective porosity model (REPM) to estimate K_s using relative effective porosity, which is defined as the ratio of effective porosity (ϕ_e) to field capacity (FC). The REPM is based on the Kozeny–Carman equation [23] and derived from the relationship between K_s and ϕ_e suggested by

Ahuja et al. [19] and Rawls et al. [21]. Several K_s models that are based on (ϕ_e) have been applied to generate the spatial distribution of K_s (e.g., [24,25]) and to estimate the effect of organic contents on soil properties (e.g., [26]). Compared to the K_s estimation model suggested by Ahuja [27], the REPM is more efficient because parameters in the model can be obtained from direct estimations such as field and laboratory tests. In other words, it has the advantage that the model requires only two parameters such as bulk density and field capacity. However, it is still uncertain whether the K_s values estimated from the REPM are as reasonable as those from the empirical methods based on the grain size analyses [28].

Regarding the validity of the K_s models, various methods were evaluated to assess whether the uncertainties impeded in K_s estimates were reasonable before being applied to practical studies. In field measurements of K_s Wu et al. [29] suggested a generalized solution for calculating the top-soil layer saturated hydraulic conductivity based on a single ring infiltrometer. Bagarello et al. [30] compared the solution of the single-ring infiltrometer with the two-ponding-depth infiltration method for a sandy-loam soil and concluded that it gave reasonable K_s measurements for various infiltration tests. More recently, Aiello et al. [31] carried out a comparison study between the Beerkan Estimation of Soil Transfer parameters (BEST) procedure and the method by Wu et al. [29]. They found that K_s values obtained by the BEST procedure are within a factor of two from those estimated by the Wu et al. [29] method. On the other hand, Reynolds et al. [32] conducted field infiltration measurements and laboratory soil core methods to estimate K_s for undisturbed soils and found that the different methods can produce different estimation results because of uncertainties inherent in the different measurement techniques. Similarly, Verbist et al. [33,34] stated that rock fragments in stony soils are correlated with the variability of K_s measurements because of macropores generated by rock fragments. For laboratory measurements, some K_s models were validated using statistical approaches such as regression lines fitted to various soil data. Comegna et al. [35] found that there is a strong correlation between estimated soil K_s with effective soil porosities. While Cheng and Chen [36] compared the results of the grain size analysis with those obtained from pumping tests, the comparison they performed was only between the K_s estimation methods. Therefore, in spite of being widely used, a cross-comparison among the K_s models has rarely been reported. Additionally, tracer tests have been widely used in laboratory and field studies to estimate the hydrogeological properties of small- and large-scale groundwater systems such as groundwater velocity, effective porosity, and dispersivity [37–39]. Compared to the field tracer tests, laboratory tracer experiments generally provides relatively confident results due to less uncertainties involved in controlled experiments [40]. In this study, three K_s estimation methods were compared with the results of breakthrough curve analyses based on bench-scale tracer experiments.

The main objective of this study was to investigate the characteristics of K_s estimates from the empirical methods of the grain size analysis (i.e., Hazen method and Cozeny–Karman equation) and the REPM by comparing them with those from the tracer experiments conducted for sand textured soils such as coarse, medium, and fine sand soils.

2. Materials and Methods

2.1. Preparation of Soil Materials

In order to perform laboratory experiments, sandy materials were sampled from the hyporheic zone of the Han River in Seoul, South Korea in 2004. The sampled materials used for the experiments were coarse, medium, and fine sand. They were collected by sieving the sampled sandy soils. The grading curve of the sandy soil was obtained by sieve analysis following the standard American Society for Testing and Materials (ASTM) procedures. As shown in Figure 1, the soil sample consists dominantly of sand (95.3%), with minor amounts of gravel (0.9%) and silt (3.8%). Among the soil grains, the composition of the sandy particle was mainly coarse sand (66.6%), followed by medium sand (22.4%) and fine sand (2.4%). The grain sizes of the samples were 0.5~1 mm for coarse sand, 0.25~0.5 mm for medium sand, and 0.125~0.25 mm for fine sand. Additionally, before packing the

materials for column and bench scale tracer tests, the bulk density of each sample was measured. The samples were dried in oven at 110 °C for 24 h and the sample weights and volumes were measured a total of 15 times to take into account variations during the measurements. The mean bulk density was 1.44 (0.05) g·cm^{-3} for coarse sand, 1.43 (0.08) g·cm^{-3} for medium sand, and 1.47 (0.03) g·cm^{-3} for fine sand. The numbers in the brackets represent the standard deviation, which is less than 6% of the average values of the bulk density. Those estimated bulk densities can be generally considered as reasonable when compared to values for the general bulk densities of sandy soils, which range from 1.2 g·cm^{-3} for very loose soils to as high as 1.8 g·cm^{-3} for very tight, fine, sandy loam soils [41]. The porosity of each soil sample was determined using the ratio of the pore volume (V_v) to the bulk volume (V) (=V_v/V), which is theoretically the same as the relationship between the dry bulk density (ρ_b) and particle density (ρ_m), which is $(\rho_m - \rho_b)/\rho_m$ [12]. In this study, both soil porosity estimation methods were used to obtain reasonable values. The measured porosity was 0.44 (0.04) cm^3·cm^{-3} for coarse sand, 0.46 (0.03) cm^3·cm^{-3} for medium sand, and 0.44 (0.04) cm^3·cm^{-3} for fine sand.

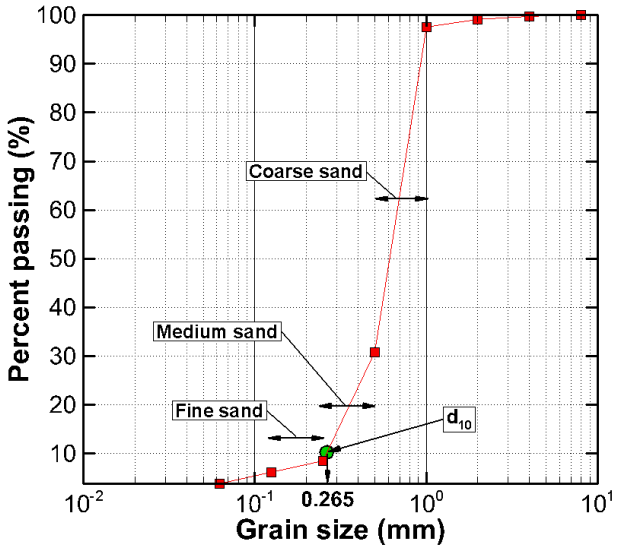

Figure 1. Particle grading curve of sandy soil samples.

2.2. Empirical Methods

Many empirical methods were developed to estimate the saturated hydraulic conductivities (K_s) of the porous materials from the grain size analysis. Based on Vuković and Soro [42], a general form of the empirical methods for estimating K_s can be expressed as:

$$K_s = \frac{\rho g}{\mu} C f(P) d_e^2 \quad (1)$$

where K_s is the saturated hydraulic conductivity [L/T], g is the gravitational constant [L/T^2], ρ is the density of fluid [M/L^3], μ is the viscosity [cP], C is the dimensionless coefficient related to physical characteristics of samples, $f(P)$ is a porosity (P) function and d_e is the effective grain diameter [L], which is generally determined by the grain size at which a 10% weight content (d_{10}) (see Figure 1). The values of C, $f(P)$, and d_e depend on the empirical models. In this study, the Hazen and Kozeny–Carman methods were used, which are widely used to calculate K_s and applicable to sand-sized material (0.125~1.0 mm). Additionally, the Hazen method is useful for the uniformly graded sand if the uniformity coefficient of a sample is less than 5, and the hydraulic conductivity can be obtained as follows [43]:

$$K_s = \frac{g}{\mu} \times 6 \times 10^{-4} \times [1 + 10(P - 0.26)] d_e^2 \quad (2)$$

where $g = 9.81$ m/s^2 and $\mu = 1.009$ cP when water is at 20 °C [44]. The Kozeny–Carman method is also one of the widely used methods when the grain size is larger than that of clayey and less than 3 mm. The saturated hydraulic conductivity based on the Cozeny–Karman Method can be expressed as follows [43]:

$$\mathrm{K_s} = \frac{g}{\mu} \times 8.3 \times 10^{-3} \times \left[\frac{P^3}{(1-P)^2}\right] d_{10}^2 \quad (3)$$

2.3. Relative Effective Porosity Model

In 2001, Suleiman and Ritchie [20] suggested a simple model for estimating $\mathrm{K_s}$ using an effective porosity of a soil, which is the relative effective porosity model (REPM) and can be written as:

$$\mathrm{K_s} = 75 \times \phi_{er}^2 \quad (4)$$

where the saturated hydraulic conductivity ($\mathrm{K_s}$) is in the unit of cm/d, and ϕ_{er} is the relative effective porosity and can be calculated by the ratio of effective porosity (ϕ_e) to field capacity (FC) as follows:

$$\phi_{er} = \frac{\phi_e}{FC} = \frac{P - \mathrm{FC}}{\mathrm{FC}} \quad (5)$$

where P is the total porosity.

In order to estimate $\mathrm{K_s}$ using the REPM, three columns packed with the coarse, medium, fine sand materials were prepared. Each column (33 cm long with an internal diameter of 10 cm) was filled with air-dried coarse, medium, or fine sand material. Once packed with the materials, the columns were saturated with tap water left open to the atmosphere for more than two days to degas chlorine to prevent air bubbles from generating between the pore spaces in the soil materials. A TRIME-FM3 Time Domain Reflectometry (TDR, IMKO Micromolutechnic GmbH, Ettlingen, Germany) was used to estimate P and FC. The P value for each column was determined by measuring the moisture contents when the soil sample was fully saturated, and FC. was determined when the moisture content changes were negligible after draining water from the columns. Before measuring the soil moisture content, the TDR was calibrated using dry glass beads and saturated glass beads [45]. The P3S rod probe was placed at depth of 11 cm below the top of the columns and the water contents of each column were measured until the difference of water contents between current and previous measurements was less than 1%. For each measurement, the moisture content was measured ten times and then the average and standard deviation of water content was calculated. In order to obtain reasonable water content values, thirteen replicates for each sample were done.

2.4. Moment Analysis and Analytical Solution for Tracer Tests

The moment analysis is generally used to interpret breakthrough curves (BTCs) obtained from laboratory and field tracer experiments (e.g., [46]). In general, the pore water velocity (mean BTC arrival time) and the dispersion coefficients can be estimated by analyzing tracer tests results with pulse or step inputs (e.g., [47,48]). The moment methods have also been applied to partitioning tracer tests to estimate non-aqueous phase liquids (NAPLs) (e.g., [49]) and convergent tracer tests to evaluate apparent dispersivity and porosity (e.g., [46]). In this study, moment methods for pulse and continuous types were applied. The pore water velocity for the pulse continuous inputs can be obtained from the following equations [47]:

$$v_p = \frac{x}{M_p - 0.5t_0};\ M_p = \frac{\int_0^\infty tC(x,t)dt}{\int_0^\infty C(x,t)dt} \quad (6)$$

where v_p is the pore water velocity [L/T], x is the distance between the injection and observation wells [L], C is the concentration, t is the time, and t_0 is the injection duration [T]. M_p is the first moment of a pulse-type breakthrough curve, which can be the center of mass arrival time (mean breakthrough

time). Similarly, for the moment method of continuous or step input, Yu et al. [48] suggested a moment method to interpret the BTCs from the step input, which has the advantage of giving reasonable results for experimental data. The pore water velocity for the continuous type (v_c) can be calculated using the first moment (M_c), which is the center of mass travel time for the continuous type (e.g., [48]), as follows:

$$v_c = \frac{x}{M_c};\ M_c = \int_0^1 tdC \tag{7}$$

Once v for both input types is obtained, the saturated hydraulic conductivity of a porous material can be calculated using Darcy's equation:

$$\mathrm{K_s} = \frac{n_e v}{i} \tag{8}$$

where n_e is the effective porosity and i is the hydraulic gradient, n_e and i can be obtained from column and tracer tests, respectively.

As another method for analyzing the breakthrough curves obtained in this study, the breakthrough curve matching was also applied to determine the transport parameters (e.g., [50]). Specifically, the breakthrough curves were analyzed by inverse curve fitting methods with CXTFIT, version 2.0 [51]. To match the curves, flux-averaged relative concentrations were assigned as an effluent type. The injected tracer was assigned to be conservative and the background concentration of the physical aquifer model was assumed to be zero. The bench-scale tracer tests were conducted under various conditions to obtain reasonable hydraulic parameters such as hydraulic conductivities and linear velocities for the coarse, medium, and fine sand materials. In general, one-dimensional (1D) column experiments are relatively simple and cost-effective methods compared to two-dimensional (2D) tank experiments. However, in some cases, 1D column experiments may produce early breakthrough and tailing of breakthrough curves [52]. Because of the various experiment conditions (e.g., tracer injection rates and volumes) applied for the tracer tests, the 2D tank experiment was selected to obtain reasonable breakthrough curves. The estimated saturated hydraulic conductivities for each soil material were compared with those estimated from the empirical and the REPM methods. The tracer tests were conducted in an acrylic tank (1 cm thick) with dimensions of 79 × 18 × 58 cm (length × width × height) as shown in Figure 2. The material setting for the experiment tank consisted of coarse, medium, and fine sand layers with a thickness of 15 cm each. Clayey layers (2 cm thick) were embedded within the two sand layers to prevent interaction between adjacent layers. Additionally, a 2-cm thick clay layer was overlain by a coarse sand layer to prevent the preferential flow along the bottom plate (Figure 2b). The hydraulic gradient of the aquifer tank was 6.33×10^{-3}, which was maintained with the water level of two reservoirs (15 × 18 × 59 cm) at the both side ends of the tank; the water level was 52.5 cm at the left side and 52.0 cm at the right side.

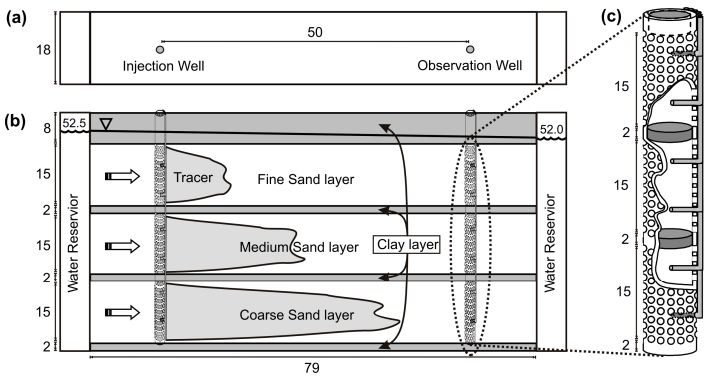

Figure 2. Setup of tank experiment: (**a**) Plan view; (**b**) Cross-section; (**c**) Well description (units in cm).

Injection and observation wells were installed in the up- and down-gradient directions, respectively. The distance between the wells was 50 cm and the injection and observation wells were located about 15 and 14 cm away from left and right reservoirs, respectively. Both of the wells were made of 0.1-cm thick Teflon pipe with an inner diameter of 1.1 cm. The wells were divided into three parts, 2~17 cm, 19~34 cm, and 36~51 cm, which were the same as the vertical distributions of sand layers to prevent interaction between the parts within the wells. To separate the well into three parts, plastic rods with dimensions of 1.0 × 2.0 cm (outer diameter × height) were placed at 0~2 cm, 17~19 cm, 34~36 cm, and 51~53 cm above the bottom of the aquifer model. Two sampling tubes were attached to each layer to inject or sample the tracer (Figure 2c).

Potassium bromide (KBr) was used as a conservative tracer and injected into the injection well. According to Mastrocicco et al. [53], saline tracers including NaBr, LiBr, NaCl, LiBr, KBr and KCl may cause errors in concentration measurements because of cation exchange interactions with soil matrix. Among the saline solutions, KBr is one of the solutions that can lead to the least measurement errors. Bromide concentrations were measured using a bromide ion-selective electrode following the guideline procedures in Orion Research Inc. [54]. To maintain its reproducibility, the bromide electrode was calibrated every two hours with a calibration standard solution of 0.1 M NaBr. In order to avoid disturbing the steady state flow condition of the sand layers, the tracer test was performed at one layer at a time. After the tracer injection was done, a total of 20 mL of degassed tap water was injected to the same layer as a chaser, which flushed the injected tracer remain in the well. The conditions applied for the tracer experiments are listed in Table 1. Two types of the tracer injection were conducted: continuous and pulse types. For the continuous-type injection, the injected volume was about 2000 mL, which was ten times larger than the injected volume for the pulsed-type injection. Because of the relatively large amount of tracer, the injection rate for each sand layer was set below 1 mL/min and thus, the tracer injection did not affect the constant flow fields maintained by the reservoir at right side of the tank (Tests 1-1, 2-1, and 3-1). For the pulsed-type injection, the tracer was injected with a rate from 5.18 to 6.25 mL/min. The volume of the injected tracer was set to 100~500 mL for coarse (Tests 1-2, 1-3, 1-4, and 1-7) and medium sand layers (Tests 2-2, 2-3, 2-4, and 2-7). With a tracer volume of 200 mL, various injection rates were applied from 1.60 to 10.39 mL/min for the coarse sand layer (Tests 1-4, 1-5, and 1-6) and 1.36 to 8.53 mL/min for the medium sand layer (Tests 2-4, 2-5, and 2-6). For the fine sand layer, two different injection volumes were applied with different injection rates. Tests 3-2 and 3-3 are comparable to Tests 1-4 and 2-4 and Tests 1-7 and 2-7, respectively.

Table 1. Tracer test conditions applied to materials.

Test No.	Test Material	Injection Type	Total Test Volume (mL)	Injection Rate (mL/min)	Initial Concentration (C_0, g·L^{-1})
1-1	C	Continuous	2000	0.66	0.049
1-2	C	Pulse	500	6.25	0.101
1-3	C	Pulse	300	5.57	0.101
1-4	C	Pulse	200	5.70	0.097
1-5	C	Pulse	200	1.60	0.096
1-6	C	Pulse	200	10.39	0.101
1-7	C	Pulse	100	5.77	0.083
2-1	M	Continuous	2000	0.61	0.049
2-2	M	Pulse	500	5.22	0.097
2-3	M	Pulse	300	5.18	0.101
2-4	M	Pulse	200	5.20	0.097
2-5	M	Pulse	200	1.36	0.091
2-6	M	Pulse	200	8.53	0.095
2-7	M	Pulse	100	5.40	0.083
3-1	F	Continuous	2000	0.59	0.047
3-2	F	Pulse	500	5.20	0.083
3-3	F	Pulse	200	1.31	0.140

Notes: C: Coarse sand layer; M: Medium sand layer; F: Fine sand layer.

3. Results and Discussion

3.1. Empirical Methods Based on Grain Size Analysis

The K_s estimations of the soil samples were conducted using the empirical methods based on grain size distributions. The parameter values (e.g., porosity and bulk density) for the empirical methods were determined by averaging estimated values based on ten replications. Table 2 lists the parameter values used for the K_s estimations. Since the grain size range for the samples was narrow, the minimum and maximum grain sizes of each sample were applied for d_{10} in the empirical methods and thus the minimum and maximum values of the soil K_s were obtained. For the Hazen method, the estimated minimum and maximum K_s values were 20.96 and 104.81 cm/min for the coarse sand material, 5.68 and 27.08 cm/min for the medium sand, and 1.31 and 6.99 cm/min for the fine sand sample, respectively. The K_s estimates using the Kozeny–Carman method were 21.48 and 161.33 cm/min for the coarse sand, 6.65 and 44.66 cm/min for the medium sand, and 1.34 and 12.35 cm/min for the fine sand. The estimated K_s using the Kozeny–Carman method were approximately 1.5 to 1.7 times higher than those obtained by the Hazen method.

Table 2. Estimated parameter values for the empirical methods.

Parameter	Coarse	Medium	Fine
Particle size (mm)	0.5~1.0	0.25~0.5	0.125~0.25
d_{10} (mm)	0.5 [a], 1.0 [b]	0.25 [a], 0.5 [b]	0.125 [a], 0.25 [b]
Porosity ($cm^3 \cdot cm^{-3}$)	0.44 [c] (0.04 [d])	0.46 [c] (0.03 [d])	0.44 [c] (0.04 [d])
Bulk density ($g \cdot cm^{-3}$)	1.44 [c] (0.05 [d])	1.43 [c] (0.08 [d])	1.47 [c] (0.03 [d])
K_s (Hazen, cm/min)	20.96 [a], 104.81 [b]	5.68 [a], 27.08 [b]	1.31 [a], 6.99 [b]
K_s (Kozeny–Carman, cm/min)	21.48 [a], 161.33 [b]	6.65 [a], 44.66 [b]	1.34 [a], 12.35 [b]

Notes: [a] minimum; [b] maximum; [c] mean; [d] standard deviation.

3.2. Column Drainage Tests for the REPM

During the water drainage tests, water contents for the samples were measured to estimate effective porosities and field capacities for obtaining K_s based on the REPM. To obtain reasonable estimates, all the experiments were repeated three times and the water contents were also measured repeatedly to characterize the variability of water contents at each measurement. Figure 3 shows the temporal changes of the water contents for the soil samples during the water drainage tests. At each time, the minimum and maximum values of the water contents were excluded when the mean and standard deviation values of the water contents were calculated. Overall, the mean water contents of the samples decreased with increasing experiment time. The standard deviation of the water contents varied from 1.2% to 2.6% for the coarse sand, 0.7% to 2.3% for the medium sand, and 0.9% to 2.8% for the fine sand soil. Because the maximum difference between the estimated K_s falls generally within the range of one order of magnitude, the variations of water contents are considered to be reasonably small for estimating the K_s estimations. As the particle size increased, the changes in the mean soil water contents were significant during the first day of the measurements, but water content changes decreased after one day. At the initial stage, the volumetric water contents were 22.3~29.6% for coarse sand, 30.8~33.9% for medium sand, and 34.2~40.0% for fine sand, which represent the saturated water contents of the soil samples. At about 0.2 days after the water drainage tests started, the water contents decreased drastically to 12.4~17.3% for the coarse sand, 20.4~26.7% for the medium sand, and 30.5~33.2% for the fine sand. In addition, there were large variations in water contents during the first day of observation (Period A in Figure 3), but the variations of the measured water contents decreased as the experiment continued (Period B in Figure 3).

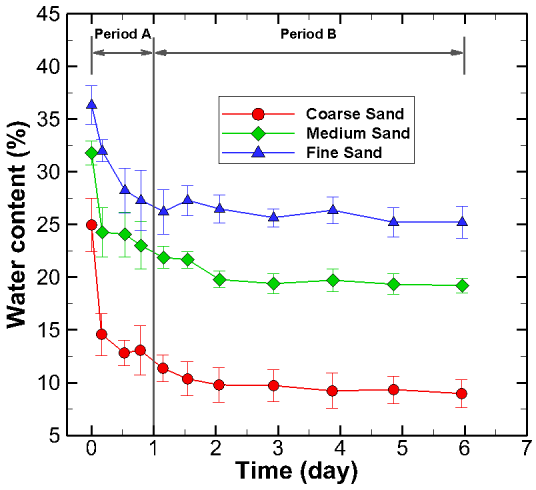

Figure 3. Temporal changes of the measured water contents (symbols and bars represent mean and standard deviation of the water contents, respectively).

For the REPM, FC is used to determine the K_s of the samples. In order to determine FC based on the temporal changes of the water contents, the approaches used by Ahuja et al. [27] and Suleiman and Ritchie [20] were used. Specifically, Ahuja et al. [27] used water contents measured at 2 days and Suleiman and Ritchie [20] used water contents measured at 2 and 3 days of free drainage tests. Therefore, the drainage test duration applied in this study was in the range from 2 to 3 days. Regarding the reasonability of determining the water contents for FC, we analyzed the water content changes with time. Since FC is defined as the amount of water content held in soil, the water content change rates of the soil samples were calculated to choose reasonable FCs:

$$\theta_t = \frac{\Delta\theta}{\Delta t} \tag{9}$$

where θ_t is the water content change rate at time t. Figure 4 shows that the estimated θ_t varies largely until the first day of drainage (Period A in Figure 4) and then approaches to zero (Period B in Figure 4), which indicates that the water content did not change with time at around 2 days after the experiment started. Therefore, we used the water contents measured at approximately 2~3 days as the FC of each soil sample because the mean change rates for all the samples were less than 4%/day.

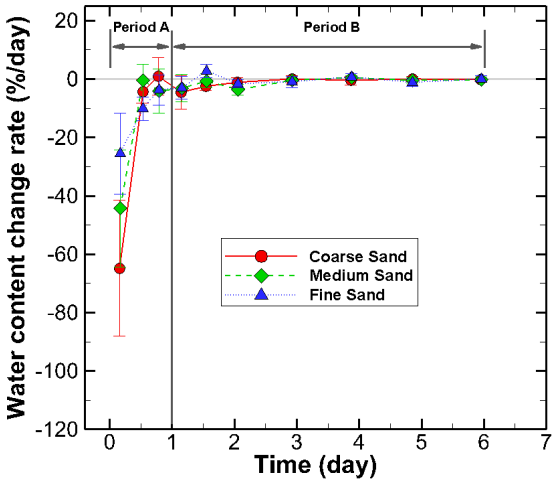

Figure 4. Water content change rates (bars represent the maximum and minimum values).

The estimated FCs for the coarse, medium, and fine sand soils ranged from 7.3% to 12.0%, 19.0% to 21.3% and 25.3% to 26.8%, respectively. The FC values used for the REPM were determined based on five to six repeated measurements. The mean and standard deviation of the measured FC are listed in Table 3. The mean FC tends to increase with decreasing grain sizes. For K_s estimation, the FC values were used to obtain the ranges of K_s for each sample. Additionally, we used the minimum and maximum porosities that were applied for the empirical methods. After substituting the measured FCs and porosities of each material into Equations (4) and (5), the variations of the estimated K_s values were analyzed. The K_s values of sand materials ranged from 0.30 to 1.44 cm/min, with a mean of 0.69 cm/min for coarse sand; from 0.05 to 0.11 cm/min, with a mean of 0.08 cm/min for medium sand; and from 0.01 to 0.04 cm/min, with a mean of 0.03 cm/min for fine sand (Table 3). Based on the standard deviations of the samples, the variation of the estimated K_s values for the coarse sand are relatively high compared to the medium and fine sand soils because of a relatively large variation of the FC that was a standard deviation of 1.8%. However, the changes of the estimated K_s were less than 50% of the mean value. In other words, the estimated K_s values for all the samples were within an order of magnitude.

Table 3. Estimated parameter values for the relative effective porosity model (REPM).

Parameter	Coarse	Medium	Fine
Field capacity (FC, %)	9.8 [a] (1.8 [b])	19.8 [a] (0.1 [b])	25.8 [a] (0.6 [b])
K_s (cm/min)	0.69 [a] (0.34 [b])	0.08 [a] (0.02 [b])	0.03 [a] (0.01 [b])

Notes: [a] mean; [b] standard deviation.

3.3. Breakthrough Curve Analyses from Bench-Scale Tracer Tests

For the tracer tests, the mean peak arrival times of breakthrough curves for coarse, medium, and fine sand layers were 841, 1282 and 7060 min, respectively. The peak concentration of the fine sand layer was relatively low because the dispersivity for the fine sand was larger than those for the coarse and medium sand soils. The estimated dispersivity values for the coarse, medium, and fine sand soils were 0.53, 0.26, and 0.63 cm, respectively. The lowest dispersivity for the medium sand resulted in the highest magnitude for the peak, and the others were in the order of coarse sand then fine sand layer. The same results were obtained for the case where the injection volume was 200 mL (breakthrough curves for Tests 1-4, 1-5, 1-6, 2-4, 2-5, 2-6, and 3-2 in Figure 5). Regarding the volume of tracer injection, it was found that the lengths of the breakthrough curve were proportional to the tracer injection volumes, but the peak arrival times of the breakthrough curves obtained from different injection volumes were similar each other: the peak arrival times ranged from 790 to 970 min for the coarse sand, 1220 to 1430 min for the medium sand, and 6890 to 7220 min for the fine sand material.

For the tracer tests in the fine sand layer, Test 3-1 was performed with a continuous tracer injection, with a similar injection rate to those for the coarse and medium sand layers (i.e., Tests 1-1 and 2-1). The peak of the relative concentration was higher than those for Tests 1-1 and 2-1, but the center-of-mass arrival time was relatively high compared to Tests 1-1 and 2-1 because of the low hydraulic conductivity for the fine sand layer. Test 3-2 was conducted with an injection rate of 5.20 mL/min. Additionally, the breakthrough curve for Test 3-2 showed a high concentration peak, but a similar arrival time to Test 3-3. Based on the results of tracer tests under the various tracer injection conditions, the breakthrough curves did not show any strong correlation with tracer injection rates. The higher concentration peak yielded a later peak arrival time when the tracer injection volume was the same, but the differences between the peak arrival times for each material were within 15%. Therefore, the calculated center of mass arrival times for continuous and pulsed types were also within similar ranges.

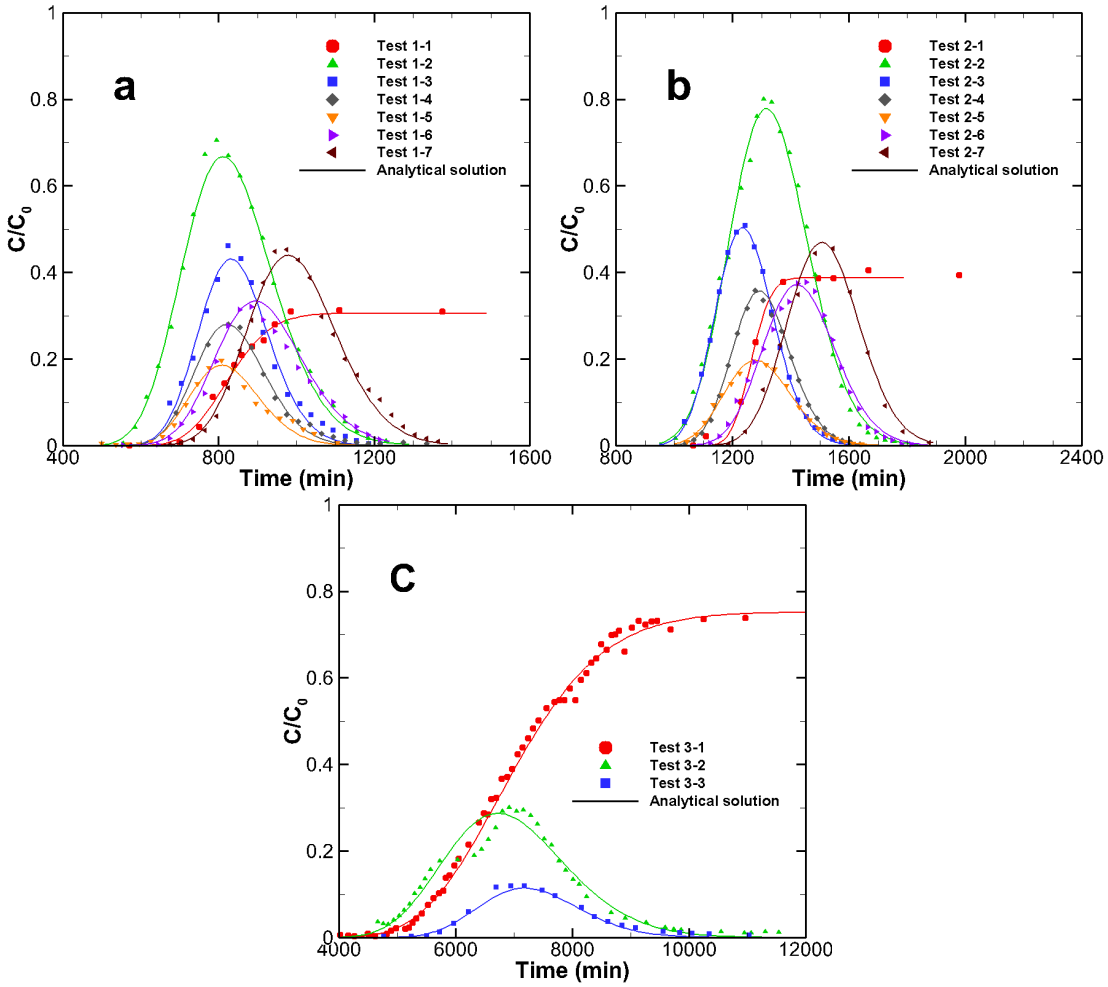

Figure 5. Breakthrough curves for (**a**) coarse, (**b**) medium and (**c**) fined sand soil layers.

The breakthrough curves obtained from the various tracer tests were analyzed using two methods: moment analysis and one-dimensional (1D) analytic solution. Based on the moment analysis, the estimated linear velocities for the coarse sand layer ranged from 5.0×10^{-2} to 6.3×10^{-2} cm/min. For the medium sand layer, the pore water velocity estimates ranged from 3.5×10^{-2} to 4.1×10^{-2} cm/min. For the fine sand layer, those estimated values were in a range from 6.8×10^{-3} to 7.5×10^{-3} cm/min. Using the 1D analytical solution, the estimated ranges of linear velocities for the coarse, medium and fine sand layers were from 5.1×10^{-2} to 6.4×10^{-2} cm/min, with a 95% confidence interval of 5.4×10^{-2} to 6.1×10^{-2} cm/min, 3.5×10^{-2} to 4.1×10^{-2} cm/min, with a 95% confidence interval of 3.6×10^{-2} to 3.9×10^{-2} cm/min, and 6.9×10^{-3} to 7.5×10^{-3} cm/min, with a 95% confidence interval of 6.8×10^{-3} to 7.5×10^{-3} cm/min, respectively. The estimated pore water velocities for the three sand layers were compared between the two methods to evaluate whether the estimates were appropriate or not. Figure 6 shows the estimated linear velocities for the sand materials from the moment analysis and the analytical solution. For the results of pore water velocity estimations, the residual sum of square (R^2) is 0.99, which indicates that the results of the analytical solution match well with those of the moment analysis and thus the linear velocities are reasonably estimated.

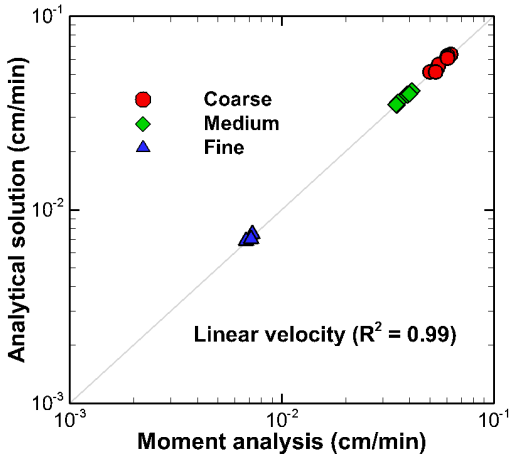

Figure 6. Comparison between the results of analytical solution and moment analysis: Pore water velocity (cm/min).

Regarding the estimated linear velocities using the breakthrough curve analyses, the K_s of each sample was calculated using the Darcy's law. To avoid a bias in estimating K_s for the samples, all possible variabilities of the input values including linear velocity and effective porosity were considered in the calculation. Specifically, the linear velocity values used in the K_s calculation were based on the results of the breakthrough curve analyses. The effective porosities applied for calculating K_s were the mean, minimum, and maximum values and they were obtained by taking the difference between the porosities and the field capacities of the samples, which were the same as those used for the empirical and REPM methods (Table 4). The hydraulic gradient applied for the calculation was 6.33×10^{-3}. The results of K_s calculations for the soil samples in Table 4 show that the mean K_s increases with grain sizes. Specifically, the mean K_s for the coarse sand is approximately two times higher than the medium sand and 15 times higher than the fine sand soil.

Table 4. Estimated mean and standard deviation of parameters for the breakthrough curve analyses.

Parameter	Coarse	Medium	Fine
Linear velocity (cm/min)	5.8×10^{-2} [a] (4.4×10^{-3} [b])	3.8×10^{-2} [a] (2.4×10^{-3} [b])	7.2×10^{-3} [a] (2.8×10^{-4} [b])
Effective porosity ($cm^3 \cdot cm^{-3}$)	3.6×10^{-1} ($\pm 3.0 \times 10^{-2}$) [c]	2.6×10^{-1} ($\pm 3.0 \times 10^{-2}$) [c]	2.1×10^{-1} ($\pm 3.0 \times 10^{-2}$) [c]
K_s (cm/min)	3.18 [a] (0.33 [b])	1.45 [a] (0.19 [b])	0.21 [a] (0.03 [b])

Notes: [a] mean; [b] standard deviation; [c] range for minimum and maximum values.

3.4. Comparison of Estimated Saturated Hydraulic Conductivities

The saturated hydraulic conductivities estimated using the empirical methods, the REPM, and breakthrough curve analyses, were compared as shown in Figure 7. The K_s values estimated based on the empirical methods range approximately from 20.96 to 188.83 cm/min for the coarse sand, 5.68 to 54.96 cm/min for the medium sand, and 1.31 to 12.35 cm/min for the fine sand. The K_s estimates obtained from the REPM and the breakthrough curve analyses were approximately one and two orders of magnitude lower than those from the empirical methods. The mean estimates of the K_s based on the breakthrough curve analyses were 3.18 cm/min (0.33) for the coarse sand, 1.45 cm/min (0.19) for the medium sand, and 0.21 cm/min (0.03) for the fine sand (numbers in parentheses correspond to standard deviation). The mean saturated hydraulic conductivity obtained using the REPM was approximately 0.79 cm/min (0.32), 0.08 cm/min (0.03), and 0.03 cm/min (0.02) for the coarse, medium, and fine sand soils, respectively. The relative variations of the estimated K_s from the breakthrough curve analyses were the smallest among the three methods, while the empirical methods produced the highest relative variation in the estimation results. Regarding the relative difference of the mean K_s values between the methods, the estimation results based on empirical methods showed approximately

26 times for the coarse sand, 16 times for the medium sand and 25 times for the fine sand greater than those based on the breakthrough curve analyses. The REPM estimated approximately 4 times for the coarse sand, 19 times for the medium sand, and 7 times for the fine sand less than the breakthrough curve analyses.

Based on the comparison results, it was found that there was a consistent trend for the estimation results, in that the estimates from the REPM were consistently lower than those obtained from the empirical methods and breakthrough curve analyses, and those from empirical methods were relatively higher than other methods. The breakthrough curve analyses gave K_s estimates between the estimates from the empirical methods and the REPM. Cheng and Chen [36] reported that the saturated hydraulic conductivities obtained from the empirical methods were relatively lower than those estimated by pumping tests. Additionally, Reynolds et al. [32] and Verbist et al. [34] suggested that different estimation methods can increase the variability of estimation results due to uncertainties associated to the estimations (e.g., rock fragments and cracks in materials). The results in this study showed that the empirical methods overestimated the saturated hydraulic conductivities when compared to those derived from the tracer test analyses. Based on the comparison, although underestimating the K_s values for the sandy soils, the REPM provided relatively similar estimates compared to those from the empirical methods because the differences of the mean values between the REPM and the breakthrough curve analyses were less than one order of magnitude except for the medium sand.

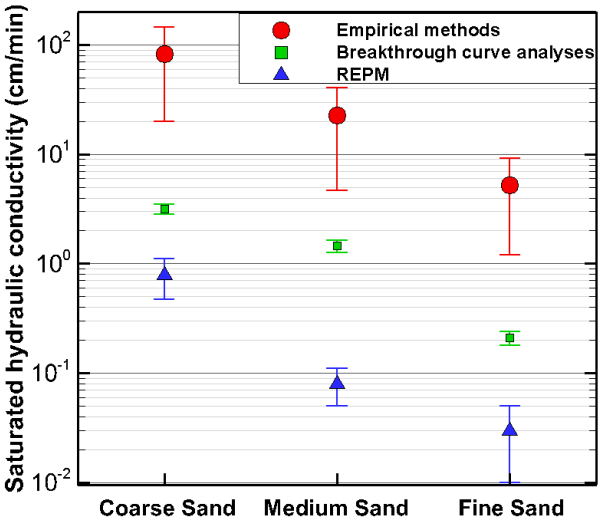

Figure 7. Comparison of the estimated saturated hydraulic conductivities among the empirical methods, the REPM and analytical solution and breakthrough curve analyses. Symbols and Bars represent means and standard deviations, respectively.

4. Conclusions

To quantify groundwater flow in the near surface, the saturated hydraulic conductivity of a soil is an important parameter that affects the variably-saturated flow in the vadose zone as well as shallow groundwater system. There are various methods for estimating the saturated hydraulic conductivities of soils, which are empirical methods based on grain size distributions and the relative effective porosity model (REPM). In this study, the estimation results from two methods were compared to those obtained from tracer tests consisting of various tracer input conditions.

Three types of sandy soils including coarse, medium, and fine sand materials were characterized using the grain size analyses for empirical methods such as Hazen and Kozeny–Carman methods, by which the saturated hydraulic conductivity of a soil can be obtained based on the grain size analysis. Compared to the results from the breakthrough curve analyses, the empirical methods gave relatively higher estimates for all the soil samples. The difference of the mean values between the empirical

methods and the breakthrough curve analyses was greater than one order of magnitude. For the coarse sand, the saturated hydraulic conductivity estimated from the empirical method was approximately 26 times greater than those from the breakthrough curve analyses. The estimation results from the REPM showed that the saturated hydraulic conductivities are consistently lower than those from the breakthrough curve analyses. The maximum difference occurs for the medium sand, which was approximately 19 times less than those from the breakthrough curve analyses. For the other sand soils, the mean values estimated from the REPM were approximately 4 times for the coarse sand and 7 times for the fine sand lower than those from the breakthrough curve analyses. Based on the comparison results, it is recommended to perform cross-validations for hydraulic conductivities estimated using one method with those estimated with other methods to obtain reasonable estimation results. Additionally, the K_s estimation methods based on neural network analyses such as Rosetta has great potential for future work on cross-validation.

Acknowledgments: This research was supported by the "R&D Project on Environmental Management of Geologic CO_2 Storage" from the KEITI (Project Number: 2014001810003).

Author Contributions: Hyoun-Tae Hwang and Kang-Kun Lee conceived and designed the experiments; Hyoun-Tae Hwang performed the experiments; Hyoun-Tae Hwang, Kang-Kun Lee, Sung-Wook Jeen and Ayman A. Suleiman analyzed the data; Hyoun-Tae Hwang, Sung-Wook Jeen, Ayman A. Suleiman and Kang-Kun Lee wrote the paper.

Conflicts of Interest: The authors declare no conflicts of interest.

References

1. Frind, E.O.; Pinder, G.F. Galerkin solution of the inverse problem for aquifer transmissivity. *Water Resour. Res.* **1973**, *9*, 1397–1410. [CrossRef]
2. Freeze, R.A.; Cherry, J.A. *Groundwate*; Prentice-Hall: Englewood Cliffs, NJ, USA, 1979.
3. Kitanidis, P.K.; Vomvoris, E.G. A geostatistical approach to the inverse problem in groundwater modeling (steady state) and one-dimensional simulations. *Water Resour. Res.* **1983**, *19*, 677–690. [CrossRef]
4. Yeh, W.W.G. Review of parameter identification procedures in groundwater hydrology: The inverse problem. *Water Resour. Res.* **1986**, *22*, 95–108. [CrossRef]
5. Arnold, J.G.; Allen, P.M.; Bernhardt, G. A comprehensive surface-groundwater flow model. *J. Hydrol.* **1993**, *142*, 47–69. [CrossRef]
6. Haitjema, H.M. *Analytic Element Modeling of Groundwater Flow*; Academic Press: San Diego, CA, USA, 1995.
7. Pinder, G.F. *Groundwater Modeling Using Geographical Information Systems*; John Wiley & Sons: New York, NY, USA, 2002.
8. Suleiman, A.A. Modeling daily soil water dynamics during vertical drainage using the incoming flow concept. *Catena* **2008**, *73*, 312–320. [CrossRef]
9. Šimůnek, J.; van Genuchten, M.T.; Šejna, M. Development and applications of the hydrus and stanmod software packages and related codes. *Vadose Zone J.* **2008**, *7*, 587–600. [CrossRef]
10. Schaap, M.G.; Leij, F.J.; van Genuchten, M.T. Rosetta: A computer program for estimating soil hydraulic parameters with hierarchical pedotransfer functions. *J. Hydrol.* **2001**, *251*, 163–176. [CrossRef]
11. Chapuis, R.P. Predicting the saturated hydraulic conductivity of soils: A review. *Bull. Eng. Geol. Environ.* **2012**, *71*, 401–434. [CrossRef]
12. Fetter, C.W. *Applied Hydrogeology*; Prentice-Hall: Upper Saddle River, NJ, USA, 2000.
13. Rawls, W.; Brakensiek, D. A procedure to predict green and ampt infiltration parameters. In Proceedings of the American Society of Agricultural Engineers Conference on Advances in Infiltration, Chicago, IL, USA, 12–13 December 1983; pp. 102–112.
14. Minasny, B.; McBratney, A.B.; Bristow, K.L. Comparison of different approaches to the development of pedotransfer functions for water-retention curves. *Geoderma* **1999**, *93*, 225–253. [CrossRef]
15. Pachepsky, Y.A.; Rawls, W. Accuracy and reliability of pedotransfer functions as affected by grouping soils. *Soil Sci. Soc. Am. J.* **1999**, *63*, 1748–1757. [CrossRef]
16. Schaap, M.G.; Leij, F.J. Database-related accuracy and uncertainty of pedotransfer functions. *Soil Sci.* **1998**, *163*, 765–779. [CrossRef]

17. Parasuraman, K.; Elshorbagy, A.; Si, B.C. Estimating saturated hydraulic conductivity using genetic programming. *Soil Sci. Soc. Am. J.* **2007**, *71*, 1676–1684. [CrossRef]
18. Bagarello, V.; Iovino, M.; Tusa, G. Factors affecting measurement of the near-saturated soil hydraulic conductivity. *Soil Sci. Soc. Am. J.* **2000**, *64*, 1203–1210. [CrossRef]
19. Ahuja, L.R.; Naney, J.W.; Green, R.E.; Nielsen, D.R. Macroporosity to characterize spatial variability of hydraulic conductivity and effects of land management1. *Soil Sci. Soc. Am. J.* **1984**, *48*, 699–702. [CrossRef]
20. Suleiman, A.; Ritchie, J. Estimating saturated hydraulic conductivity from soil porosity. *Trans. ASAE* **2001**, *44*. [CrossRef]
21. Rawls, W.J.; Brakensiek, D.; Saxtonn, K. Estimation of soil water properties. *Trans. ASAE* **1982**, *25*, 1316–1320. [CrossRef]
22. Timlin, D.; Ahuja, L.; Pachepsky, Y.; Williams, R.; Gimenez, D.; Rawls, W. Use of brooks-corey parameters to improve estimates of saturated conductivity from effective porosity. *Soil Sci. Soc. Am. J.* **1999**, *63*, 1086–1092. [CrossRef]
23. Carman, P. Fluid flow through granular beds. *Chem. Eng. Res. Des.* **1997**, *75*, S32–S48. [CrossRef]
24. Ahuja, L.R.; Cassel, D.K.; Bruce, R.R.; Barnes, B.B. Evaluation of spatial distribution of hydraulic conductivity using effective porosity data. *Soil Sci.* **1989**, *148*, 404–411. [CrossRef]
25. Regalado, C.M.; Muñoz-Carpena, R. Estimating the saturated hydraulic conductivity in a spatially variable soil with different permeameters: A stochastic kozeny–carman relation. *Soil Tillage Res.* **2004**, *77*, 189–202. [CrossRef]
26. Nemes, A.; Rawls, W.J.; Pachepsky, Y.A. Influence of organic matter on the estimation of saturated hydraulic conductivity. *Soil Sci. Soc. Am. J.* **2005**, *69*, 1330–1337. [CrossRef]
27. Ahuja, L.R.; Wendroth, O.; Nielsen, D.R. Relationship between initial drainage of surface soil and average profile saturated conductivity. *Soil Sci. Soc. Am. J.* **1993**, *57*, 19–25. [CrossRef]
28. Anderson, M.P.; Woessner, W.W.; Hunt, R.J. *Applied Groundwater Modeling: Simulation of Flow and Advective Transport*; Academic press: San Diego, NJ, USA, 2015.
29. Wu, L.; Pan, L.; Mitchell, J.; Sanden, B. Measuring saturated hydraulic conductivity using a generalized solution for single-ring infiltrometers. *Soil Sci. Soc. Am. J.* **1999**, *63*, 788–792. [CrossRef]
30. Bagarello, V.; Sferlazza, S.; Sgroi, A. Comparing two methods of analysis of single-ring infiltrometer data for a sandy–loam soil. *Geoderma* **2009**, *149*, 415–420. [CrossRef]
31. Aiello, R.; Bagarello, V.; Barbagallo, S.; Consoli, S.; Di Prima, S.; Giordano, G.; Iovino, M. An assessment of the beerkan method for determining the hydraulic properties of a sandy loam soil. *Geoderma* **2014**, *235–236*, 300–307. [CrossRef]
32. Reynolds, W.D.; Bowman, B.T.; Brunke, R.R.; Drury, C.F.; Tan, C.S. Comparison of tension infiltrometer, pressure infiltrometer, and soil core estimates of saturated hydraulic conductivity. *Soil Sci. Soc. Am. J.* **2000**, *64*, 478–484. [CrossRef]
33. Verbist, K.; Baetens, J.; Cornelis, W.M.; Gabriels, D.; Torres, C.; Soto, G. Hydraulic conductivity as influenced by stoniness in degraded drylands of chile. *Soil Sci. Soc. Am. J.* **2009**, *73*, 471–484. [CrossRef]
34. Verbist, K.M.J.; Cornelis, W.M.; Torfs, S.; Gabriels, D. Comparing methods to determine hydraulic conductivities on stony soils. *Soil Sci. Soc. Am. J.* **2013**, *77*, 25–42. [CrossRef]
35. Comegna, V.; Damiani, P.; Sommella, A. Scaling the saturated hydraulic conductivity of a vertic ustorthens soil under conventional and minimum tillage. *Soil Tillage. Res.* **2000**, *54*, 1–9. [CrossRef]
36. Cheng, C.; Chen, X. Evaluation of methods for determination of hydraulic properties in an aquifer–aquitard system hydrologically connected to a river. *Hydrogeol. J.* **2007**, *15*, 669–678. [CrossRef]
37. LeBlanc, D.R.; Garabedian, S.P.; Hess, K.M.; Gelhar, L.W.; Quadri, R.D.; Stollenwerk, K.G.; Wood, W.W. Large-scale natural gradient tracer test in sand and gravel, cape cod, massachusetts: 1. Experimental design and observed tracer movement. *Water Resour. Res.* **1991**, *27*, 895–910. [CrossRef]
38. Wagner, B.J.; Harvey, J.W. Experimental design for estimating parameters of rate-limited mass transfer: Analysis of stream tracer studies. *Water Resour. Res.* **1997**, *33*, 1731–1741. [CrossRef]
39. Garabedian, S.P.; LeBlanc, D.R.; Gelhar, L.W.; Celia, M.A. Large-scale natural gradient tracer test in sand and gravel, cape cod, massachusetts: 2. Analysis of spatial moments for a nonreactive tracer. *Water Resour. Res.* **1991**, *27*, 911–924. [CrossRef]
40. Yang, Y.; Lin, X.; Elliot, T.; Kalin, R. A natural-gradient field tracer test for evaluation of pollutant-transport parameters in a porous-medium aquifer. *Hydrogeol. J.* **2001**, *9*, 313–320. [CrossRef]

41. Weil, R.R.; Brady, N.C.; Weil, R.R. *The Nature and Properties of Soils*; Pearson: Columbus, OH, USA, 2016.
42. Vuković, M.; Soro, A. *Determination of Hydraulic Conductivity of Porous Media from Grain-Size Composition*; Water Resources Pubns: Littleton, CO, USA, 1992.
43. Odong, J. Evaluation of empirical formulae for determination of hydraulic conductivity based on grain-size analysis. *J. Am. Sci.* **2007**, *3*, 54–60.
44. William Lambe, T. *Soil Testing for Engineers*; John Wiley and Sons, Inc.: London, UK, 1951.
45. IMKO Micromodultechnik GmbH. *Trime-fm User Manual*; IMKO Micromodultechnik GmbH: Ettlingen, Germany, 2001.
46. Fernandez-Garcia, D.; Sánchez-Vila, X.; Illangasekare, T.H. Convergent-flow tracer tests in heterogeneous media: Combined experimental–numerical analysis for determination of equivalent transport parameters. *J. Contam. Hydrol.* **2002**, *57*, 129–145. [CrossRef]
47. Wolff, H.-J.; Radeke, K.-H.; Gelbin, D. Heat and mass transfer in packed beds—iv: Use of weighted moments to determine axial dispersion coefficients. *Chem. Eng. Sci.* **1979**, *34*, 101–107. [CrossRef]
48. Yu, C.; Warrick, A.; Conklin, M. A moment method for analyzing breakthrough curves of step inputs. *Water Resour. Res.* **1999**, *35*, 3567–3572. [CrossRef]
49. Jin, M.; Delshad, M.; Dwarakanath, V.; McKinney, D.C.; Pope, G.A.; Sepehrnoori, K.; Tilburg, C.E.; Jackson, R.E. Partitioning tracer test for detection, estimation, and remediation performance assessment of subsurface nonaqueous phase liquids. *Water Resour. Res.* **1995**, *31*, 1201–1211. [CrossRef]
50. Das, B.; Wraith, J.; Kluitenberg, G.; Langner, H.; Shouse, P.; Inskeep, W. Evaluation of mass recovery impacts on transport parameters using least-squares optimization and moment analysis. *Soil Sci. Soc. Am. J.* **2005**, *69*, 1209–1216. [CrossRef]
51. Toride, N.; Leij, F.; Van Genuchten, M.T. *The CXTFIT Code for Estimating Transport Parameters from Laboratory or Field Tracer Experiments*; U. S. Salinity Laboratory: Riverside, CA, USA, 1995; Volume 2.
52. Rabideau, A.J.; Van Benschoten, J.; Patel, A.; Bandilla, K. Performance assessment of a zeolite treatment wall for removing sr-90 from groundwater. *J. Contam. Hydrol.* **2005**, *79*, 1–24. [CrossRef] [PubMed]
53. Mastrocicco, M.; Prommer, H.; Pasti, L.; Palpacelli, S.; Colombani, N. Evaluation of saline tracer performance during electrical conductivity groundwater monitoring. *J. Contam. Hydrol.* **2011**, *123*, 157–166. [CrossRef] [PubMed]
54. Thermo Fisher Scientific. *User Guide, Bromide Ion Selective Electrode*; Thermo Fisher Scientific: Beverly, MA, USA, 2008.